Key Points:
- Quasiperiodic oscillation of equatorial electrojet waves
- Ionosphere-atmosphere coupling
- Modulation of electrojet waves by gravity waves

Correspondence to:
E. B. Shume,
Esayas.B.Shume@jpl.nasa.gov

Modulation of equatorial electrojet irregularities by atmospheric gravity waves

E. B. Shume[1], F. S. Rodrigues[2], A. J. Mannucci[1], and E. R. de Paula[3]

[1] Jet Propulsion Laboratory, California Institute of Technology, Pasadena, California, USA, [2] W. B. Hanson Center for Space Sciences, University of Texas at Dallas, Richardson, Texas, USA, [3] National Institute for Space Research, São José dos Campos, Brazil

Abstract On 9 January 2002 and 14 November 2001, the São Luís 30 MHz coherent backscatter radar observed unusual daytime echoes scattered from the equatorial electrojet. The electrojet echoing layers on these days, as seen in the range time intensity maps, exhibited quasiperiodic oscillations. Time-frequency decomposition of the magnetic field perturbations ΔH, measured simultaneously by the ground-based magnetometers, also showed evidence of short-period waves. The ground-based observations were aided by measurements of the brightness temperature in the water vapor and infrared bands made by the GOES 8 satellite. The GOES 8 satellite measurements indicated evidence of deep tropospheric convection activities, which are favorable for the launch of atmospheric gravity waves (AGW) near São Luís. Our multitechnique investigation, combined with an analysis of the equatorial electric field and current density, indicates that AGW forcing could have been responsible, via coupling with E region electric fields, for the short-period electrojet oscillations observed over São Luís.

1. Introduction

Experimental and modeling research have suggested the influences of gravity waves on the Earth's ionosphere [*Fritts and Lund*, 2011]. Atmospheric general circulation modeling studies [*Yiğit et al.*, 2009; *Yiğit and Medvedev*, 2010; *Yiğit et al.*, 2012a] and numerical simulations [*Vadas and Fritts*, 2006] demonstrate that gravity waves can propagate from the lower atmosphere into the thermosphere-ionosphere system. Radar observations of short-period fluctuations of the phase velocities of electrojet waves and electric fields were suggested to be caused by atmospheric waves [e.g., *Reddy and Devasia*, 1976; *Hysell et al.*, 1997; *Abdu et al.*, 2002; *Aveiro et al.*, 2009]. Gravity waves could modify ionospheric electric fields [*Kelley*, 2009], and they are also proposed as seeds for equatorial spread F [*Kelley et al.*, 1981; *Fritts et al.*, 2009; *Makela et al.*, 2010; *Tsunoda*, 2010].

On 9 January 2002 and 14 November 2001 (geomagnetically quiet days as indicated by the AE index in Figure 1), the São Luís (Brazil) 30 MHz radar observed unusual echoes characterized by temporal and/or spatial quasi-oscillations of the electrojet scattering layers. Horizontal magnetic field perturbations ΔH (a proxy for electrojet strength) measured over São Luís showed temporal oscillations.

In this study, we use time-frequency decomposition of the ΔH time series, analysis of brightness temperature in the water vapor and infrared bands from the GOES 8 satellite, and theoretical analysis about ionospheric electric field to investigate the physical mechanisms responsible for the quasiperiodic oscillations of the electrojet scattering layers.

2. Data Presentation
2.1. The 9 January 2002 Data
2.1.1. Coherent Scatter Radar Data (30 MHz)
The São Luís radar has been semiroutinely observing daytime E region and nighttime F region irregularities since 2000. Descriptions of the radar and examples of observations are given by *de Paula and Hysell* [2004], *Rodrigues et al.* [2008], and *Shume et al.* [2011].

Figure 2a shows the range time intensity (RTI) graph of coherent scatter echoes from electrojet irregularities received by the São Luís radar on 9 January 2002. The RTI graph shows signal-to-noise ratio (S/N in dB) of the radar echoes as a function of range and UT. The radar echoes in the fluctuating region are well above the background noise level. The integration time was 3 min. The RTI graph shows unique radar echoes
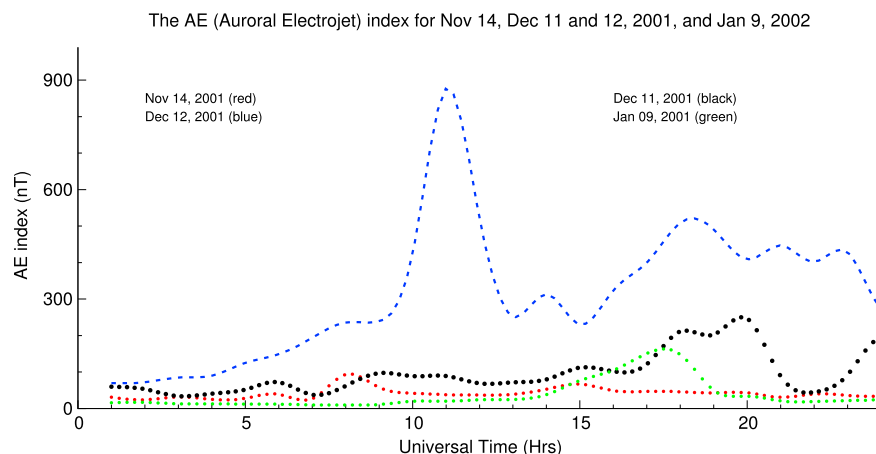
Figure 1. The auroral electrojet index (hourly) for 14 November 2001, 11 December 2001, 12 December 2001, and 9 January 2002.

exhibiting quasiperiodic oscillations (the fluctuations of the intensity (S/N) are not perfectly periodic) of the electrojet echoing layer (~12:00 to 16:00 UT). During quiet days, such oscillations are rare because the background electric field mostly overwhelms wind-driven perturbation electric fields. Figure 2a shows that the strong radar echoes are confined to a relatively narrow altitude region (~3 km). Note that the radar echo strength is highly correlated with the strength of the convection electric field that drives the irregularities [*Hysell et al.*, 2008]. For comparison, Figures 2b and 2c present radar echoes scattered from the electrojet during quiet (11 December 2001) and disturbed (12 December 2001) conditions (Figure 1 shows the *AE* index), respectively. The scattered power is disrupted from about 12:00 to 14:00 UT on 12 December (Figure 2c) due to suppression of electrojet instability by storm-induced electric fields. Finally, Figure 2d shows the RTI graph for observations made on 14 November 2001, when again quasiperiodic oscillations in the electrojet layer were observed (between 17 and 18 UT). The radar echoes in Figures 2a, 2c, and 2d have features different from what is typically observed (Figure 2b, which shows continuous echo intensities over time). Figure 2c, on the other hand, show fluctuations and even suppression of the echo intensity caused by perturbation electric fields generated during geomagnetic disturbances (see *AE* index in Figure 1). Figures 2a and 2d, however, show echo intensities that abnormally vary with time in a quasiperiodic fashion, despite geomagnetically quiet conditions.

2.1.2. Power Spectra of ΔH Data

Figure 3a plots ΔH for 9 January (red) and 1 January (black, quiet time). ΔH has 1 min resolution. The strength of the equatorial electrojet is commonly measured by ground-based magnetometers located at equatorial stations. ΔH, which is a measure of the strength of the equatorial electrojet, can be obtained by calculating the difference in magnitude of the measured horizontal magnetic field component between a magnetometer placed on the magnetic equator and one placed 6°–9° away [*Anderson et al.*, 2002; *Shume et al.*, 2010]. Accordingly, horizontal magnetic field residues ΔH at São Luís, Brazil, (2.3°S; 44.2°W; 0.5°S dip latitude) are obtained by subtracting from it magnetic field measurements at Eusébio (3.8°S; 39.4°W; 6.3°S dip latitude). Eusébio is located outside the influence of the electrojet. Nighttime baseline magnetometer records for each station are subtracted first to obtain daytime values. The baseline record is an average of midnight values of five geomagnetically quietest days in a month. Fluxgate magnetometers have very good accuracy of about 0.25% to 0.50% (A manual of fluxgate magnetometer, FRG-601G, Version 1.1, Tierra Tecnica Ltd, 2002, Tokyo). The vertical lines in Figure 3a bound the region of ΔH oscillations which are accompanied by radar echo fluctuations (Figure 2a). Between the vertical lines, the magnitude of ΔH for 9 January is depressed when compared to 1 January (quiet time example). We analyzed the ΔH signal using wavelet decomposition whose results are shown in Figure 3b as a 2-D time-frequency image. The 2-D spectra reveal the existence of ~20 to 60 min period waves in the electrojet. The 95% confidence levels are shown by the contour curves on the spectra in Figures 3b and 3d. The regions on the edges of the spectra delineated by the black dotted line show the cone of influence (where the edge effect is important). The nature of these fluctuations will be investigated next in terms of electric field perturbations.
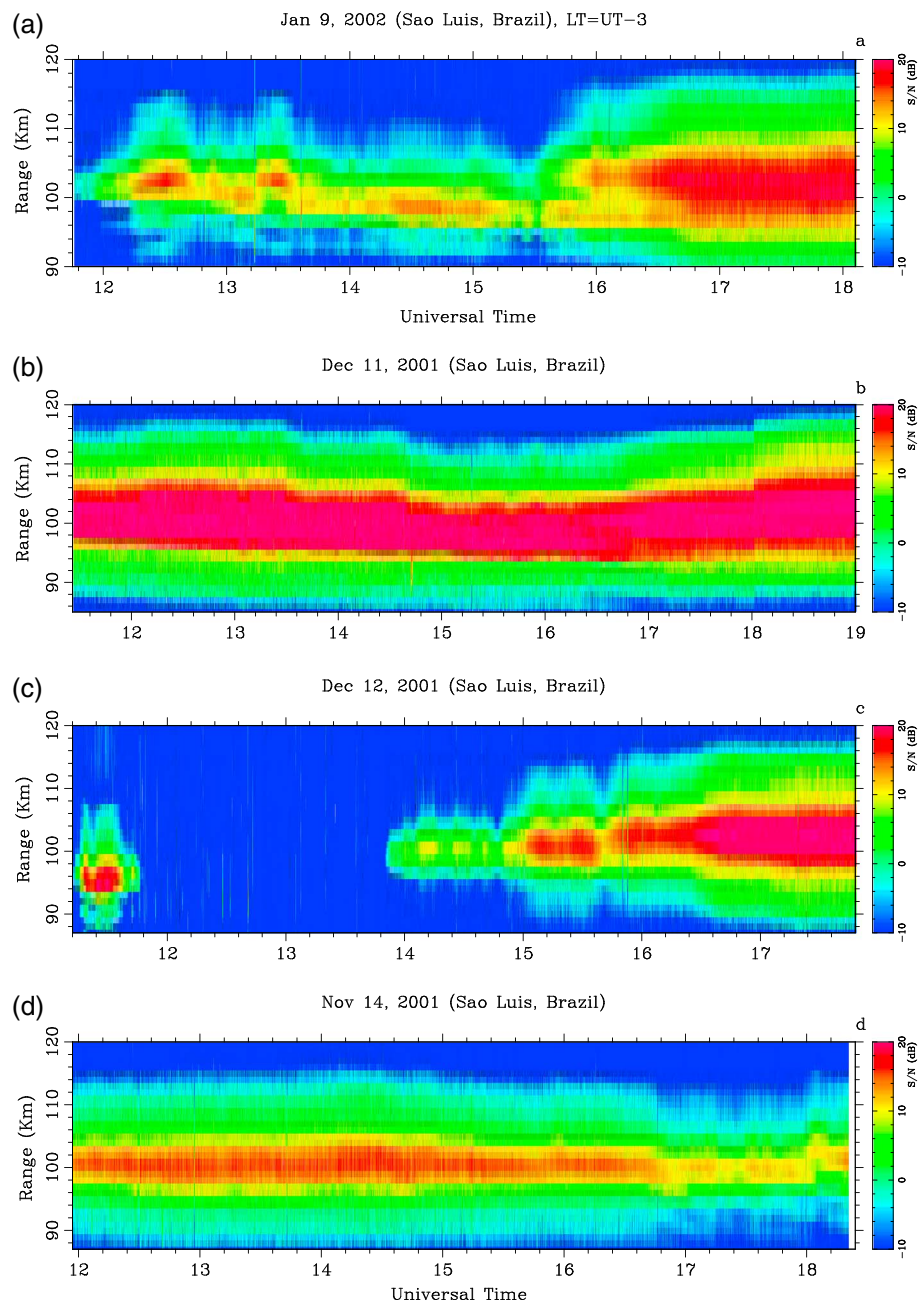
Figure 2. (a) Range time intensity (RTI) representation of coherent scatter from the equatorial electrojet irregularities received by the 30 MHz radar in São Luís on 9 January 2002. The RTI map shows signal-to-noise ratio (S/N dB) of the radar echoes (described by the legend) as a function of range and UT. (b) Same as Figure 1a but for 11 December 2001. (c) Same as Figure 1a but for 12 December 2001. (d) Same as Figure 1a but for 14 November 2001.

2.1.3. GOES 8 Satellite Brightness Temperature Images

The connection between generation of gravity waves and active convection regions have been extensively discussed in the literature [e.g., *Fritts et al.*, 2009; *Vadas et al.*, 2009]. Cold clouds near the tropopause region are indicative of regions of active convection and a likely source of gravity waves [*Vadas et al.*, 2009]. Cold brightness temperature suggests deep convective plumes and convective overshoot which are a convenient launching platform for gravity waves [*Fritts et al.*, 2009; *Vadas et al.*, 2009]. Gravity waves generated from the convective sources can propagate into the higher altitude and penetrate deep into the upper atmosphere [*Yiğit et al.*, 2008; *Fritts et al.*, 2009; *Vadas et al.*, 2009]. For cold cloud tops, the brightness temperature in the water vapor (WV) band can be higher than the infrared (IR) band (WV − IR > 0°C) [*Schmetz*
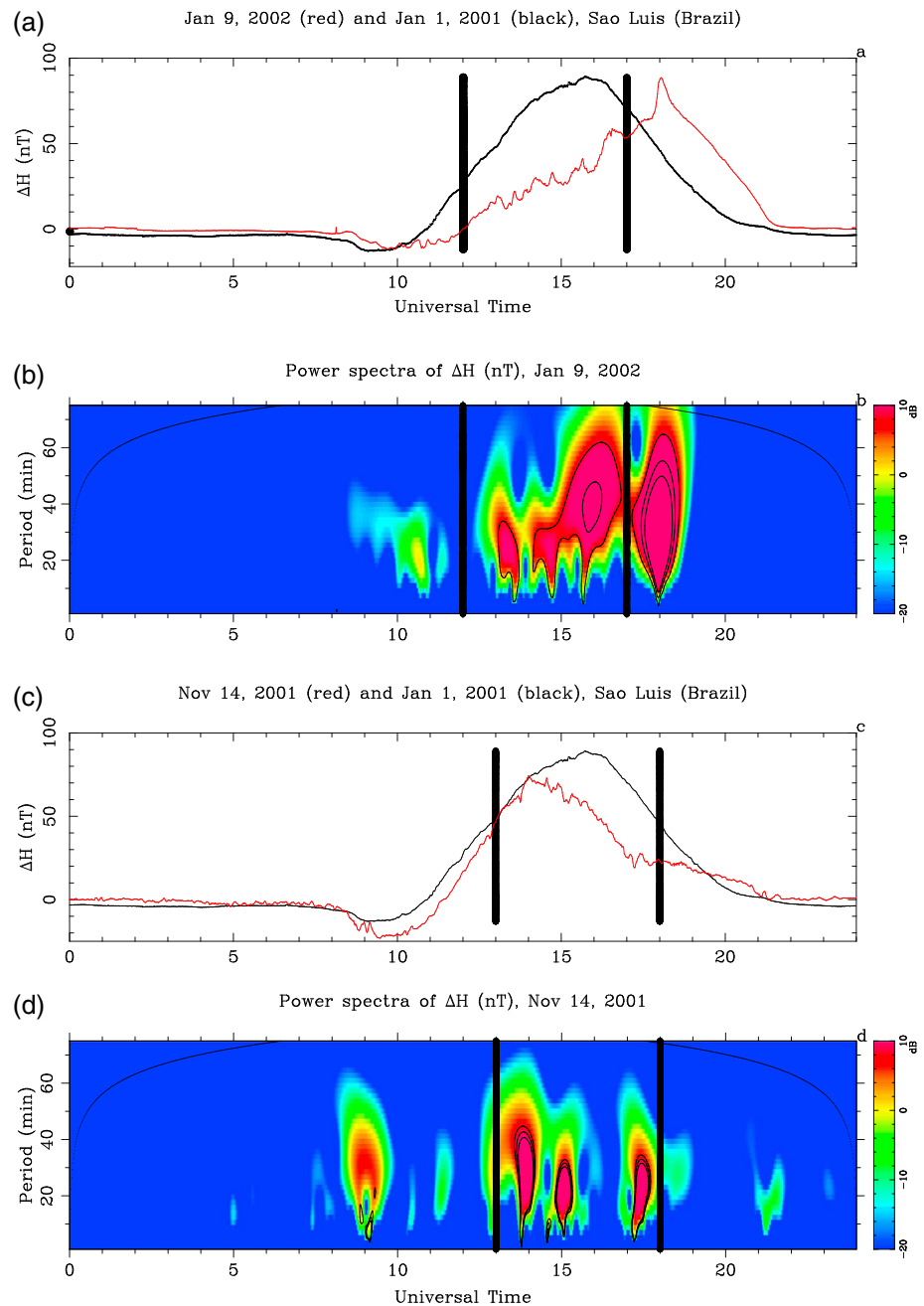
Figure 3. (a) Ground-based magnetic field perturbation ΔH in São Luís for 1 January 2001 (black) and 9 January 2002 (red). (b) Two-dimensional time-frequency power spectra of the ΔH signal for 9 January 2002. (c) Same as Figure 2a but for 14 November 2001 (red). (d) Same as Figure 2b but for 14 November 2001.

et al., 1997]. Figure 4 presents WV − IR observed by the GOES 8 satellite for selected hours on 9 January 2002 in the region of interest (São Luís is marked as a star) as a function of latitude and longitude.

In Figure 4, from about 6:15 to 12:15 UT, we observe intense convection activities (WV − IR > 0°C) within the 500 km radius north-east of São Luís suggesting possible regions of deep convective plumes and convective overshoots, a likely source of gravity waves. Example WV − IR images are shown in Figure 4. After about 12:15 UT, the figures show low convection activities (WV − IR < 0°C) north-east of São Luís indicating convection activities might have been subsided. There were, however, indicators of active convection in the south-west of São Luís (~1300 km).
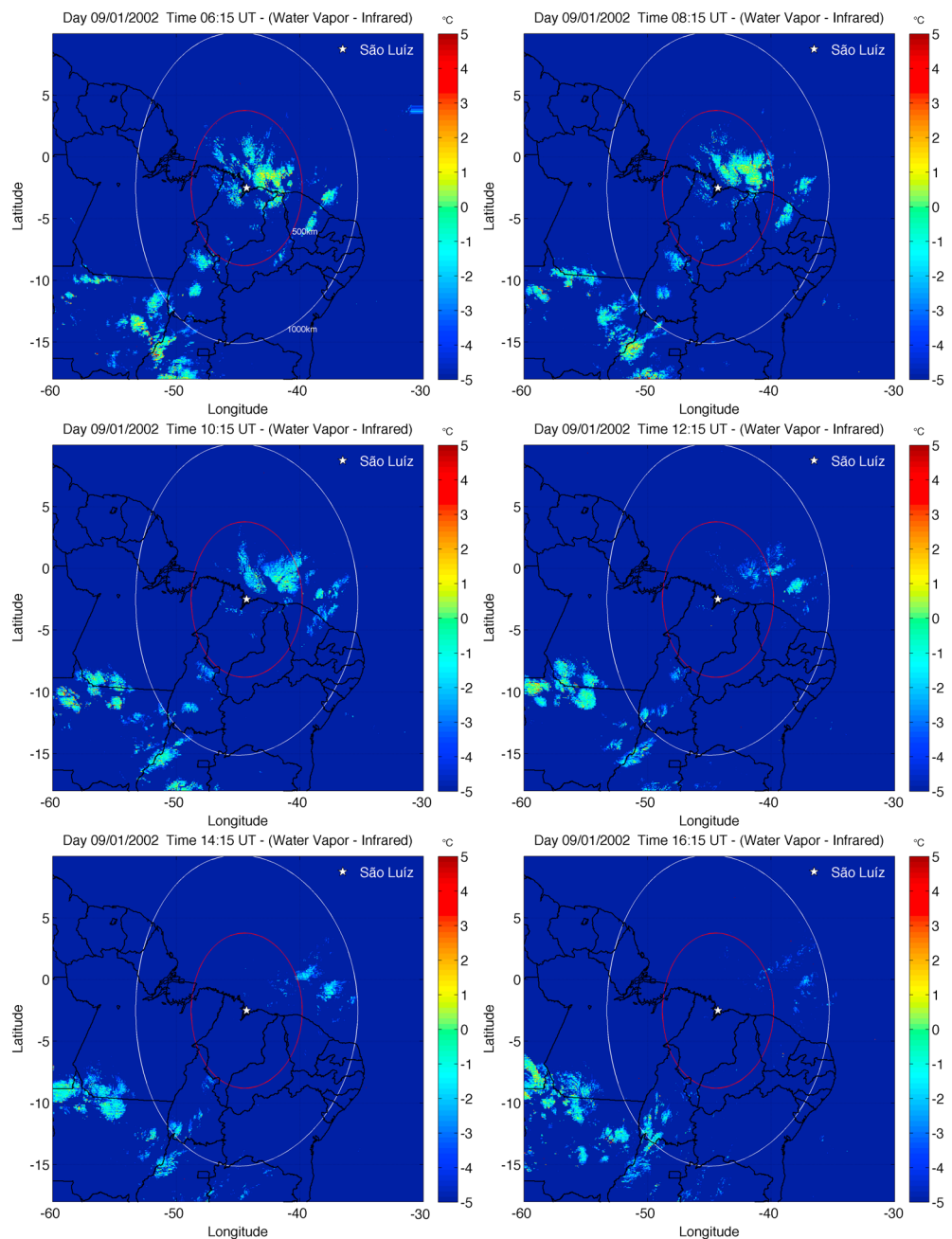
Figure 4. GOES 8 satellite data: The difference between the brightness temperature in the water vapor and infrared bands over part of South America on 9 January 2002.

Using ray tracing analysis of gravity waves detected over Brasilia by an Airglow imager, *Vadas et al.* [2009] showed that gravity waves could take ~3 to 24 h to reach dissipation altitudes (lower thermosphere). Using correlation between wind velocity measurements and convection activities over Indonesia, *Venkateswara Rao et al.* [2011] suggested that the time delay between the peak of a deep convection and propagating gravity waves in the lower thermosphere could be ~1 to 15 h. Hence, we expect gravity waves generated by the tropospheric convection (north-east and south-west of São Luís, Figure 4) to be able to modulate electrojet irregularities until ~16:00 UT (Figure 1a).

2.2. The 14 November 2001 Data
2.2.1. Coherent Scatter Radar Data (30 MHz)
This section presents additional quiet time radar data scattered from the daytime electrojet over São Luís. Figure 2d presents radar echoes scattered from the electrojet on 14 November. After ~17:00 UT, Figure 2d

shows temporal variations in the scattered power. A closer look at Figure 2d shows temporal fluctuations of the echoes from ~14:00 to 16:00 UT. After ~17:00 UT, the echo strength was lowered by ~10 dB. During this time the strongest echoes are limited to a narrow region indicating that the electric fields with the proper orientation driving the instabilities were confined to that region.

2.2.2. Power Spectra of ΔH Data

Figure 3c plots ΔH for 14 November (red). It shows fluctuating ΔH (red) from ~14:00 to 18:00 UT. Consistently the magnitude of ΔH (red) is depressed (bounded by vertical lines) when compared to a quiet time example ΔH (black). Figure 3d presents the time-frequency spectra of the ΔH signal. From ~14:00 to 18:00 UT, the spectra contain short-period waves (20–40 mins) consistent with gravity wave periods suggesting atmosphere-ionosphere coupling which could have been forced by tropospheric convection activities.

2.2.3. GOES 8 Satellite Brightness Temperature Images

Figure 5 shows GOES 8 satellite WV − IR images on 14 November (data were available every 3 h). Within 1000 km south-west of São Luiś, the images show cold cloud top temperature WV−IR > 0°C indicating deep tropospheric convection, a likely source of gravity waves. Between ~5:45 and 17:45 UT, strong convection activity happened within ~500 to 1000 km of São Luís. About 1 to 15 h would be sufficient for gravity waves to reach the E region [*Vadas et al.*, 2009; *Venkateswara Rao et al.*, 2011]. Gravity waves generated from these convection sources could have obliquely propagated to the E region to cause the radar echo fluctuations (Figure 2d) and ΔH oscillations (Figure 3c).

3. Interpretation and Discussion

The spectra in Figures 2b and 2d show short-period gravity waves, possibly originating from tropospheric convection could modulate electric fields in the electrojet. Previous general circulation modeling and numerical studies demonstrated that gravity waves of lower atmospheric origin can penetrate into the thermosphere-ionosphere system [*Yiğit et al.*, 2008, 2009; *Vadas et al.*, 2009; *Yiğit et al.*, 2012a, 2012b]. The thickness of the electrojet is typically ~25 km. This feature means that gravity waves with vertical wavelength less than 50 km are most likely interact with the background dynamo field in the electrojet and to cause electric field variations with altitude. Gravity waves with vertical wavelength >50 km marginally cause electric field variations. Ray tracing analysis has shown that gravity waves at the dissipation altitude (lower thermosphere) can have periods of ~10 to 90 min, and vertical wavelength of ~5 to 30 km [*Vadas et al.*, 2009]. Gravity waves observed over Brasilia by an Airglow imager were ray traced and found to have propagated obliquely and covered horizontal distance of ~300 to 1500 km [*Vadas et al.*, 2009]. Hence, the GOES 8 WV − IR data and the ray tracing suggest that the modulation of the radar echo strength and ΔH on 9 January and 14 November could have been potentially caused by gravity waves that propagated from tropospheric convections located at horizontal distances of within about 500 km north-east of São Luís, and within about 1500 km south-west of São Luís.

Low-frequency (long-period) gravity waves propagate nearly horizontally, and high-frequency (short-period) waves propagate close to zenith [*Vadas et al.*, 2009]. This is consistent with the spectra for 9 January (Figure 3b) and 14 November (Figure 3d). On 9 January, gravity waves which propagated from ~250 km north-east of São Luís have caused the short-period waves (~20 to 30 min, Figure 3b) from about 13 to 15 UT, and gravity waves which propagated from ~1000 km south-west of São Luís have caused the 40 to 60 min waves (15 to 16 UT, Figure 3b). On 14 November (Figure 3d), gravity waves which propagated from ~700 km south-west of São Luís caused 30 to 40 min fluctuations.

3.1. Modulation of Electric and Magnetic Fields by Winds

Assuming plasma quasi-neutrality and equipotential approximation, the vertical electric field E_α in the electrojet can be described in terms of a zonal electric field E_ϕ, a neutral wind field (u_ϕ, u_α), and conductivities σ_P (Pedersen) and σ_H (Hall) [*Hysell et al.*, 2002].

$$E_\alpha = \frac{h_\phi E_\phi \int \sigma_H h_\beta \, \mathrm{d}\beta}{h_\alpha \int \sigma_P \frac{h_\phi h_\beta}{h_\alpha} \mathrm{d}\beta} - \frac{\int \sigma_P u_\phi B_\circ h_\phi h_\beta \, \mathrm{d}\beta}{h_\alpha \int \sigma_P \frac{h_\phi h_\beta}{h_\alpha} \mathrm{d}\beta} - \frac{\int \sigma_H u_\alpha B_\circ h_\phi h_\beta \, \mathrm{d}\beta}{h_\alpha \int \sigma_P \frac{h_\phi h_\beta}{h_\alpha} \mathrm{d}\beta} \tag{1}$$

where $(h_\alpha, h_\phi, h_\beta)$ are geometric scale factors (coordinate transformation factors which keep distance invariant) and $B_\circ$ is the geomagnetic field. (α, β, ϕ) are the orthogonal dipole coordinates which are perpendicular-upward, parallel to the dipole field, and perpendicular-eastward [*Shume et al.*, 2005].
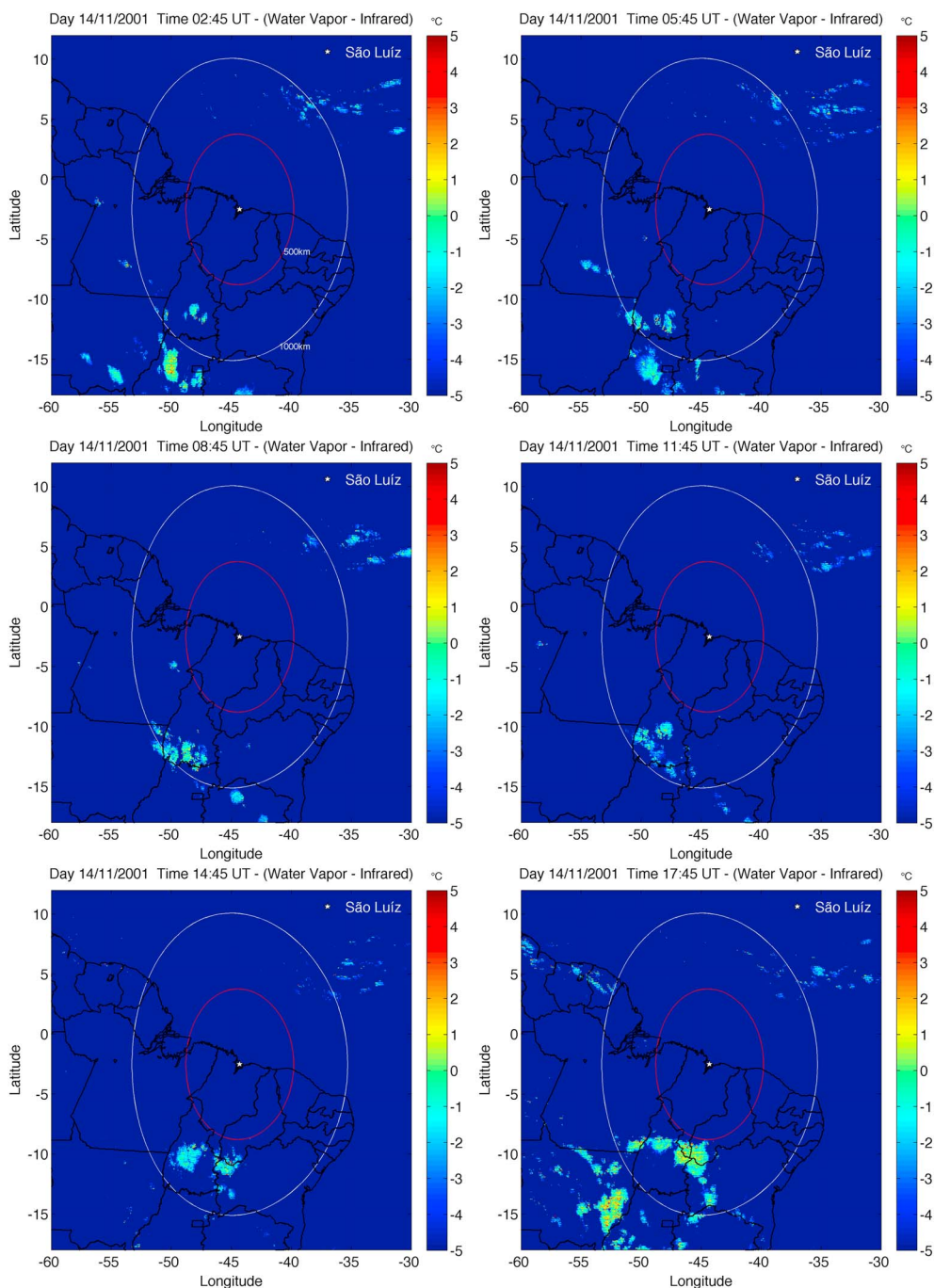
Figure 5. GOES 8 satellite data: The difference between the brightness temperature in the water vapor and infrared bands over part of South America on 14 November 2001.

The strength and orientation of ΔH is a measure of the magnitude and direction of the vertical field E_α [*Hysell et al.*, 2002]. The magnitude of ΔH for 9 January and 14 November (bounded by vertical lines) are systematically reduced compared to a representative quite time ΔH (1 January) indicating that E_ϕ has been weak in those time intervals. This creates the scenario that the wind u_ϕ driven dynamo (term 2, equation (1)) would compete with E_ϕ (term 1, equation (1)) for dominance. Note that the magnitude and direction of the dynamo field generated by winds (u_ϕ, u_α) (aggregate of the background winds and gravity wave winds (which propagated from deep tropospheric convection sources)) determine the magnitude and direction of E_α. Large wavelength electrojet waves are excited whenever E_α has positive component along positive density gradients. The strength of E_α (driving the electrojet irregularities) is strongly correlated with the radar

echo strength. In this scenario, the various phases of wind fields of short vertical wavelength ($<$ 50 km) gravity waves (terms 2 and 3, equation (1)) interact with E_ϕ (term 1, equation (1)) differently to cause a vertically varying E_α and generate the quasiperiodic irregularities (oscillating radar echoes) shown in Figures 2a and 1d.

Using equation (1), the horizontal current density (electrojet) $J_\phi = \sigma_P(E_\phi - u_\alpha B_\circ) + \sigma_H(E_\alpha + u_\phi B_\circ)$ can be expressed in terms of the background and dynamo fields:

$$J_\phi = \sigma_P E_\phi \left(1 + \frac{\sigma_H}{\sigma_P} \frac{\int \sigma_H \frac{h_\phi h_\beta}{h_\alpha} d\beta}{\int \sigma_P \frac{h_\phi h_\beta}{h_\alpha} d\beta}\right) + \sigma_H B_\circ \left(u_\phi - \frac{\int \sigma_P u_\phi \frac{h_\phi h_\beta}{h_\alpha} d\beta}{\int \sigma_P \frac{h_\phi h_\beta}{h_\alpha} d\beta}\right)$$
$$- \sigma_P B_\circ \left(u_\alpha + \frac{\sigma_H}{\sigma_P} \frac{\int \sigma_H u_\alpha \frac{h_\phi h_\beta}{h_\alpha} d\beta}{\int \sigma_P \frac{h_\phi h_\beta}{h_\alpha} d\beta}\right). \tag{2}$$

The phases of the short wavelength gravity wave (which could be polychromatic) wind fields generated by the tropospheric convective activities (Figures 4 and 5) would have their phases varying along magnetic field lines. In this case, gravity wave-induced winds (u_ϕ, term 2, equation (2)) could influence the magnitude and direction of J_ϕ. For gravity waves with constant phases along magnetic field lines, however, horizontal winds (term 2, equation (2)) would marginally influence the strength of the equatorial electrojet. In addition, large vertical winds (term 3, equation (2)) are required to influence the magnitude and direction of J_ϕ; that is, the third term should compete with the first and second terms. Driven by active tropospheric convection (Figures 4 and 5), gravity wave propagating from below could be coupled to the region and modulate the background electric field and cause the quasiperiodic oscillations in the radar echoes and ΔH.

In addition, gravity wave momentum deposition can occur much higher in the upper atmosphere [*Vadas et al.*, 2009; *Yiğit et al.*, 2008; *Yiğit and Medvedev*, 2010]. Various studies have suggested links between deep convection, gravity waves, and their likely contributions to the excitation of Rayleigh Taylor instability and plasma bubbles extending to much higher altitudes [*Fritts et al.*, 2009; *Vadas et al.*, 2009].

4. Summary and Conclusions

On 9 January 2002 and 14 November 2001, the São Luís 30 MHz radar observed unusual quasiperiodic fluctuations in the intensity of equatorial electrojet irregularity echoes. Two-dimensional decomposition of ΔH over São Luís, on these days, shows short-period waves, 20 to 60 min (9 January) and 20 to 40 min (14 November), which are considered to be evidence of atmospheric gravity wave activity. We also notice that ΔH values were lower than a quiet time example ΔH. Corresponding to those time intervals, the difference between the brightness temperature in the water vapor and infrared bands (WV − IR) observed by the GOES 8 satellite have indicated tropospheric convection activities (a launching pad for gravity waves into the upper atmosphere) in the north-east and south-west of São Luís. Driven by active tropospheric convection, gravity waves could be coupled to the electrojet and modulate the E region electric field thereby causing the fluctuating radar echoes and the ΔH oscillations observed on 9 January and 14 November.

References

Abdu, M. A., et al. (2002), Equatorial electrojet irregularities investigations using a 50 MHz back-scatter radar and a digisonde at São Luís: Some initial results, *J. Atmos. Sol. Terr. Phys.*, *64*(12-14), 1425–1434, doi:10.1016/S1364-6826(02)00106-2.

Anderson, D., A. Anghel, K. Yumoto, and M. Ishitsuka (2002), Estimating daytime vertical E×B drift velocities in the equatorial *F* region using ground-based magnetometer observations, *Geophys. Res. Lett.*, *29*(12), 1596, doi:10.1029/2001GL01562.

Aveiro, H. C., C. M. Denardini, and M. A. Abdu (2009), Climatology of gravity waves-induced electric fields in the equatorial *E* region, *J. Geophys. Res.*, *114*, A11308, doi:10.1029/2009JA014177.

de Paula, E. R., and D. L. Hysell (2004), The São Luís 30 MHz coherent scatter ionospheric radar: System description and initial results, *Radio Sci.*, *39*, RS1014, doi:10.1029/2003RS002914.

Fritts, D. C., et al. (2009), Overview and summary of the Spread *F* Experiment (SpreadFEx), *Ann. Geophys.*, *27*, 2141–2155, doi:10.5194/angeo-27-2141-2009.

Fritts, D. C., and T. S. Lund (2011), Gravity wave influences in the theromsphere and ionosphere: Observations and recent modeling, in *Aeronomy of the Earth's Atmosphere and Ionosphere*, edited by M. A. Abdu et al., IAGA Special Sopron Book Series, Springer Science, New York, doi:10.1007/978-94-007-0326-1, (to appear in print).

Hysell, D. L., M. F. Larsen, and R. F. Woodman (1997), JULIA radar studies of electric fields in the equatorial electrojet, *Geophys. Res. Lett.*, *24*(13), 1687–1690.

Hysell, D. L., J. L. Chau, and C. G. Fesen (2002), Effects of large horizontal winds on the equatorial electroject, *J. Geophys. Res.*, *107*(A8), SIA 27-1–SIA 27-12, doi:10.1029/2001JA000217.

Hysell, D. L., G. Michhue, M. F. Larsen, R. Pfaff, M. Nicolls, C. Heinselman, and H. Bahcivan (2008), Imaging radar observations of Farley Buneman waves during the JOULE II experiment, *Ann. Geophys.*, *26*, 1837–1850, doi:10.5194/angeo-26-1837-2008.

Kelley, M. C., M. Larsen, C. LaHoz, and J. McClure (1981), Gravity wave initiation of equatorial spread *F*: A case study, *J. Geophys. Res.*, *86* (A11), 9087–9100.

Kelley, M. C. (2009), *The Earth's Ionosphere: Plasma Physics and Electrodynamics*, International Geophysics Series, vol. 96, Academic Press, San Diego, Calif.

Makela, J. J., S. L. Vadas, R. Muryanto, T. Duly, and G. Crowley (2010), Periodic spacing between consecutive equatorial plasma bubbles, *Geophys. Res. Lett.*, *37*, L14103, doi:10.1029/2010GL043968.

Reddy, C. A., and C. V. Devasia (1976), Short period fluctuations of the equatorial electrojet, *Nature*, *261*, 396–397.

Rodrigues, F. S., D. L. Hysell, and E. R. de Paula (2008), Coherent backscatter radar imaging in Brazil: Large-scale waves in the bottomside *F* region at the onset of equatorial spread *F*, *Ann. Geophys.*, *26*, 3355–3364.

Schmetz, J., S. A. Tjembs, M. Gube, and L. van de Berg (1997), Monitoring deep convection and convective overshooting with Meteosat, *Adv. Space Res.*, *19*(3), 433–441.

Shume, E. B., D. L. Hysell, and J. L. Chau (2005), Zonal wind velocity profiles in the equatorial electrojet derived from phase velocities of type II radar echoes, *J. Geophys. Res.*, *110*, A12308, doi:10.1029/2005JA011210.

Shume, E. B., C. M. Denardini, E. R. de Paula, and N. B. Trivedi (2010), Variabilities of the equatorial electrojet in Brazil and Perú, *J. Geophys. Res.*, *115*, A06306, doi:10.1029/2009JA014984.

Shume, E. B., E. R. de Paula, and M. A. Abdu (2011), Modulation of equatorial electrojet plasma waves by overshielding electric field during geomagnetic storms, *J. Geophys. Res.*, *116*, A08302, doi:10.1029/2010JA016353.

Tsunoda, R. T. (2010), On equatorial spread *F*: Establishing a seeding hypothesis, *J. Geophys. Res.*, *115*, A12303, doi:10.1029/2010JA015564.

Vadas, S. L., and D. Fritts (2006), Influence of solar variability on gravity wave structure and dissipation in the thermosphere from tropospheric convection, *J. Geophys. Res.*, *111*, A10S12, doi:10.1029/2005JA011510.

Vadas, S. L., et al. (2009), Convection: The likely source of the medium-scale gravity waves observed in the OH airglow layer near Brasilia, Brazil, during the SpreadFEx campaign, *Ann. Geophys.*, *27*, 231–259, doi:10.5194/angeo-27-231-2009.

Venkateswara Rao, N., Y. Shibagaki, and T. Tsuda (2011), Diurnal variation of short-period (20–120 min) gravity waves in the equatorial Mesosphere and Lower Thermosphere and its relation to deep tropical convection, *Ann. Geophys.*, *29*, 623–629, doi:10.5194/angeo-29-623-2011.

Yiğit, E., A. D. Aylward, and A. S. Medvedev (2008), Parameterization of the effects of vertically propagating gravity waves for thermosphere general circulation models: Sensitivity study, *J. Geophys. Res.*, *113*, D19106, doi:10.1029/2008JD010135.

Yiğit, E., A. S. Medvedev, A. D. Aylward, P. Hartogh, and M. J. Harris (2009), Modeling the effects of gravity wave momentum deposition on the general circulation above the turbopause, *J. Geophys. Res.*, *114*, D07101, doi:10.1029/2008JD011132.

Yiğit, E., and A. S. Medvedev (2010), Internal gravity waves in the thermosphere during low and high solar activity: Simulation study, *J. Geophys. Res.*, *115*, A00G02, doi:10.1029/2009JA015106.

Yiğit, E., A. S. Medvedev, A. D. Aylward, A. J. Ridley, M. J. Harris, M. B. Moldwin, and P. Hartogh (2012a), Dynamical effects of internal gravity waves in the equinoctial thermosphere, *J. Atmos. Sol. Terr. Phys.*, *90-91*, 104–116, doi:10.1016/j.jastp.2011.11.014.

Yiğit, E., and A. S. Medvedev (2012b), Gravity waves in the thermosphere during a sudden stratospheric warming, *Geophys. Res. Lett.*, *39*, L21101, doi:10.1029/2012GL053812.